ESA CCI SST (v2.1)

Sea Surface Temperature (SST) from the European Space Agency Climate Change Initiative (ESA CCI)

1. Intent of This Document and Point of Contact

1a. This document summarizes essential information needed for using the ESA CCI SST data in climate applications. References are provided at the end of this document to additional information.

Dataset File Name: **tos_mon_ESA-CCI-SST-v2-1_BE_gn_198109-201712.nc**

1b. Technical point of contact for this dataset:

Name: Christopher J Merchant

E-mail: c.j.merchant@reading.ac.uk

Skype: cjmerchant

2. Data Field Description

CF variable name and units:	*sea_surface_temperature* (K)
Spatial resolution:	1.0° latitude-longitude grid
Temporal resolution and extent:	Monthly averaged, from 01/10/1981 to 31/12/2017
Coverage:	Global oceans excluding sea-ice, on full-globe grid. All longitudes. Latitude range with data approximately -78°S to 85°N

3. Data Origin

3a. Source

The data covering 1981 to 2016 come from the Sea Surface Temperature (SST) project of the European Space Agency's Climate Change Initiative (ESA CCI), derived from the v2.1 outputs of this project [1]. The data for 2017 were generated using the same approach but under funding of the Copernicus Climate Change Service.

The data are obtained from post-processing of >4 trillion individual skin sea surface temperature (SST-skin) retrievals from infra-red imagery of sensors on Earth observing satellites. The main post-processing steps are:

- the addition to the SST-skin of adjustments to daily-mean SST at a nominal depth of 20 cm, resulting in an estimate of "SST-depth"
- the uncertainty-weighted combination of SST-depth values from all the sensors to make a daily-gap-free SST analysis at 0.05° latitude-longitude resolution
- the averaging and uncertainty propagation from the daily SST analysis to monthly 1° data

In the processing, ERA-Interim fields [2] are used as ancillary information with minimized influence on the SST outcome. Consistent fields of sea ice fraction and sea fraction are also provided. The sea ice fraction is obtained from the Ocean and Sea-Ice Satellite Application

Facility [1,4] and the sea fraction accounts for ice from the same product and also the presence or not of land in the cell, determined from a surface classification dataset [5].

3b. Simplified processing steps

For a high-level but comprehensive description see [1].

1. Pre-processing of level 1b geolocated calibrated infra-red images from the series of Advanced Very High Resolution Radiometers (AVHRRs, "4 km" global data) and Along-track scanning radiometers (ATSRs, "1 km" global data).

2. Cloud detection, where pixels in satellite image are eliminated if their probability of being cloud-affected exceeds a threshold. This is done at full resolution. After cloud detection the mean density of good-quality observations is 13 km^{-2} yr^{-1}.

3. Inversion from clear-sky BTs to skin SSTs at full resolution, with associated estimation of SST uncertainty due to radiometric noise and intrinsic retrieval error.

4. Estimation of 20 cm depth SSTs at a time of day representative of the daily mean, using skin and stratification models driven by ERA-Interim surface fluxes.

5. Averaging clear-sky pixel SSTs to 0.05° resolution cells, keeping day and night separate, keeping different sensors separated, and calculating SST uncertainty per cell.

6. Ingestion of data from all sensors into a variational analysis to blend data and fill gaps. The feature resolution of the analysis is around 20 km [6]. Sea-ice information is also ingested.

7. Averaging of the SST, propagation of the SST uncertainty, averaging of sea ice and sea fractions, into the monthly 1° resolution of the obs4MIPs version.

3c. Assumptions and use of prior data

SST-skin retrieval is wholly independent of in situ SST observations for the ATSR series and nearly independent for the AVHRR series, except prior to 1993, where in situ SSTs are used as a calibration reference. The weak dependence of the AVHRR series on in situ SSTs after 1993 arises because some information (<20% for best quality data used here) is derived from use of ERA-Interim fields, which are created by data assimilation of all types of observations.

Adjustment to SST-depths involves modeling the surface skin effect and diurnal variability, using models forced by ERA-interim flux and wind fields.

3d. Merging data of more than one instrument

Observations are merged across a total of 14 sensors that have been referenced (after 1993) using satellite overlaps to Advanced ATSR. Prior to 1993, consistency is from referencing to in situ SSTs (drifting buoy and ship records).

Merging accounts fully for the diurnal cycle in SST: the artefacts that would arise from sampling at different times of day through the record are reduced by the step of adjusting SST-skin to SST-depth at a representative time of day.

3e. Sampling used in creating the source gridded product

SSTs are obtained for all clear-sky pixels in images with nominally 1 km to 4 km nadir resolution. These full resolution results are gridded to 0.05° for ingestion to the analysis. The relative uncertainty (sensor and datum specific) and the sampling uncertainty from any incomplete number of pixels contributing to a 0.05° cell are used by the analysis to weight observations appropriately.

3f. Spatial and temporal averaging used in creating the final gridded product

Around 10^4 SST retrievals contribute to each 1° monthly average value of SST on average. The density is generally higher later in the record and lowest during the 1980s, when uncertainties are correspondingly higher.

4. Validation and Uncertainty Estimate

Product verification, in situ validation and product user assessment exercises have been undertaken and are described in project reports of SST CCI [7,8,9] at the level of the swath (L2P), gridded (L3) and analysed (L4) CCI SST products. Direct validation of monthly 1° averages has not been undertaken.

4a. Assessment of mean (systematic) errors

The target for the dataset is for mean errors to be less than 0.1 K on 1000 km scales. This has been rigorously demonstrated for AATSR SST-skin values against in situ radiometer measurements (mean difference being, in fact, <0.01 K); however, radiometric validation is possible only for the more recent sensors. Monthly global-mean and zonal-mean comparison of SST-depth with drifting buoys suggests (to the extent that this in situ network is unbiased) that mean error <0.1 K is mostly achieved on global and zonal scales for both ATSR and AVHRR sensor series from around 1994 onwards (figure 1, middle and lower panel). Prior to that, a combination of post-Pinatubo stratospheric aerosol conditions and fewer, older sensors means that global mean errors are <0.2 K from the mid 1980s to 1994. Prior to 1985, the sparse distribution of drifting buoys with potentially larger uncertainty makes the accuracy harder to assess by this means, although our judgement is that it is likely to remain of the order a couple of tenths of kelvin. Exceptions are the following periods, associated with sensor problems, during which there are biases not accounted for within the stated uncertainties that introduce artefacts in the global-mean CCI analysis SST. During these periods, there are global mean biases appearing to be in the range of 0.1 to 0.5 K: May 1982, October to December 1982, early August 1983 and late September 1983. A further known accuracy artefact is unscreened and unadjusted-for desert dust events that cause intermittent negative biases of magnitude 1 K in CCI AVHRR SSTs in the north east tropical Atlantic, Red Sea and Gulf of Arabia; the sensitivity of ATSR-series sensors to these events is much less, but nonetheless the AVHRR problems do influence the all-sensor averages.

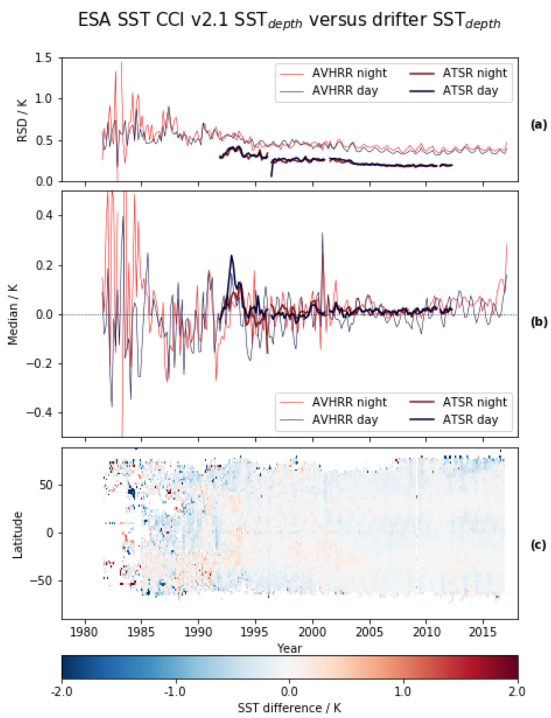

Figure 1. Global-mean by sensor-series (a, b) and zonal-mean all-sensors (c) monthly SST-depth minus drifting-buoy SST.

4b. Evaluation of uncertainty

Uncertainty per SST datum is provided in all ESA SST CCI products, in line with recommended practice [10]. These account for instrument noise, retrieval uncertainty, sub-sampling uncertainty (representativeness) and uncertainty from variational analysis (including gap filling). Unaccounted for sources of error include outbreaks of elevated desert dust and some "bad running" of sensors, which cause errors larger than expected from the quoted uncertainties in a minority of locations and times (see previous section).

The obs4MIPs uncertainty estimate approximately accounts for error correlation in the SST CCI analysis, which has a strong correlation over 3 days and on the synoptic scales of the atmosphere (i.e., strong correlation across a 1° area). The uncertainty provided for a 1° monthly average is evaluated from the daily 0.05° SST CCI analysis uncertainty estimates under the conservative assumption of perfect error correlation over 3 days and 1°. Letting the indices of CCI analysis SSTs within a cell with respect to latitude, longitude and time (day) be i, j and d respectively, the provided (total) uncertainty estimate is (expressed for an all-sea cell and a month containing n_{days} days):

$$\sqrt{\frac{3}{n_{days}} \sum_{d=1}^{n_{days}} \left(\frac{1}{20^2} \sum_{i=1}^{20} \sum_{j=1}^{20} u_{i,j,d} \right)^2}$$

Away from coasts and dynamic regions, uncertainty <0.1 K is typical.

4c. Assessment of stability

The multi-annual global observational stability (actually, instability) for the time series, relative to drifting buoy SSTs is, with 95% confidence, in the range -0.0026 to 0.0004 K yr^{-1}, assessed using the techniques of [11]. The observational instability of the drifting buoy network should be combined with the above to give an overall assessment of stability, but we do not have an estimate for this. The exception to the above figure is in the region of intermittent desert dust around north Africa: the larger sensitivity of the SST CCI analysis to dust outbreaks prior to the ATSR series in the 1990s means that multi-decadal trends including the 1980s will include a significant positive (warming trend) artefact in that geographical area.

5. Considerations for Model-Observation Comparisons

The sampling of the diurnal cycle has been adjusted such that any risk of aliasing the diurnal cycle into long-term changes has been minimized. The data represent a UTC-daily mean.

SST observations are only made for clear-sky scenes, therefore the data sample only cloud-free viewing conditions. The implications of this for representativity uncertainty in a monthly-mean SST-depth estimate are not fully clear, but are not thought to be significant.

Data gaps for any given month are the result of satellite swath limitations and exclusion of cloudy areas. Despite lower coverage than for other satellite datasets such as AVHRR, there is evidence that SST variability associated with phenomena such as ENSO is cleanly captured.

The data have larger uncertainty in the 1980s.

Times and places subject to errors beyond what is expected from the given uncertainty estimates include specific periods in the 1980s and areas of significant desert dust loading: see section 4 for details.

When publishing any paper or report using the data, users are requested to cite reference [1] and the obs4MIPs dataset reference. The data may be described to as "monthly 1° averages of SSTs from the ESA SST CCI analysis v2.1".

6. Instrument Overview

ATSRs were designed specifically to deliver SSTs of a quality relevant to climate. ATSRs are dual-view radiometers, by virtue of along-track scanning, which provides a greater information content for SST and atmospheric variability than a single view. They have two onboard high-accuracy black bodies for improved calibration over the range of SST relevance. Active cooling of detectors gives low noise at pixel level (of order 5 cK). The AVHRRs are single view sensors with similar channels to the ATSRs. AVHRRs were not intended for climate applications and in order to create this CDR, we are attempting to use these instruments well beyond their specifications for uncertainty and stability, using data-improvement techniques and metrological analysis [12].

7. References

1. Merchant, Christopher J., Owen Embury, Claire E. Bulgin, Thomas Block, Gary Corlett, Emma Fiedler, Simon A. Good, Jonathan Mittaz, Nick A. Rayner, David Berry, Steinar Eastwood, Michael Taylor, Yoko Tsushima, Alison Waterfall, Ruth Wilson and Craig Donlon. Satellite-based time-series of sea-surface temperature since 1981 for climate applications. Scientific Data **6**, 223. https://doi.org/10.1038/s41597-019-0236-x (2019)
2. Dee, D. P., Uppala, S. M., Simmons, A. J., Berrisford, P. , Poli, P. , Kobayashi, S. , Andrae, U. , Balmaseda, M. A., Balsamo, G. , Bauer, P. , Bechtold, P. , Beljaars, A. C., van de Berg, L. , Bidlot, J. , Bormann, N. , Delsol, C. , Dragani, R. , Fuentes, M. , Geer, A. J., Haimberger, L. , Healy, S. B., Hersbach, H. , Hólm, E. V., Isaksen, L. , Kållberg, P. , Köhler, M. , Matricardi, M. , McNally, A. P., Monge-Sanz, B. M., Morcrette, J. , Park, B. , Peubey, C. , de Rosnay, P. , Tavolato, C. , Thépaut, J. & Vitart, F. The ERA-Interim reanalysis: configuration and performance of the data assimilation system. *Q.J.R. Meteorol. Soc.*, **137**, 553-597. https://doi.org/10.1002/qj.828 (2011).
3. EUMETSAT Ocean and Sea Ice Satellite Application Facility. *Global sea ice concentration climate data record 1979-2015*(v2.0, 2017), [Online]. Norwegian and Danish Meteorological Institutes. doi: 10.15770/EUM_SAF_OSI_0008
4. Lavergne, T., Sørensen, A. M., Kern, S., Tonboe, R., Notz, D., Aaboe, S., Bell, L., Dybkjær, G., Eastwood, S., Gabarro, C., Heygster, G., Killie, M. A., Brandt Kreiner, M., Lavelle, J., Saldo, R., Sandven, S., and Pedersen, L. T.: *Version 2 of the EUMETSAT OSI SAF and ESA CCI sea-ice concentration climate data records*, The Cryosphere, 13, 49-78, doi:10.5194/tc-13-49-2019, 2019.
5. Carrea, L., Embury, O. and Merchant, C. J. (2015) Datasets related to in-land water for limnology and remote sensing applications: distance-to-land, distance-to-water, water-body identifier and lake-centre co-ordinates. Geoscience Data Journal, 2 (2). pp. 83-97. ISSN 2049-6060 doi: https://doi.org/10.1002/gdj3.32
6. Fiedler, E. K., Mao, C., Good, S. A., Waters, J., Martin, M. J.: Improvements to feature resolution in the OSTIA sea surface temperature analysis using the NEMOVAR assimilation scheme. Quarterly Journal of the Royal Meteorological Society, 145(725), 3609–3625, doi:10.1002/qj.3644, 2019.
7. SST-CCI Product Validation Plan (PVP) SST_CCI-PVP-UOL-001, Issue 2, 4 February 2014, available at https://climate.esa.int/projects/sea-surface-temperature/SST-key-documents/.

8. SST-CCI System Verification Report (SVR) SST_CCI-SVR-BC-202, Issue 1, 9 October 2019, available at https://climate.esa.int/projects/sea-surface-temperature/SST-key-documents/ .
9. SST-CCI Climate Assessment Report (CAR), SST_CCI-CAR-UKMO-20, Issue 1, 16 June 2019, available at https://climate.esa.int/projects/sea-surface-temperature/SST-key-documents/.
10. Merchant, C. J., Paul, F., Popp, T., Ablain, M., Bontemps, S., Defourny, P., Hollmann, R., Lavergne, T., Laeng, A., de Leeuw, G., Mittaz, J., Poulsen, C., Povey, A. C., Reuter, M., Sathyendranath, S., Sandven, S., Sofeiva, V. F. and Wagner, W. (2017) Uncertainty information in climate data records from Earth observation. Earth System Science Data, 9 (2). pp. 511-527. ISSN 1866-3516 doi: https://doi.org/10.5194/essd-9-511-2017
11. Berry, D. I., Corlett, G. K., Embury, O. and Merchant, C. J. (2018) Stability assessment of the (A)ATSR sea surface temperature climate dataset from the European Space Agency Climate Change Initiative. Remote Sensing, 10 (1). 126. ISSN 2072-4292 doi: https://doi.org/10.3390/rs10010126
12. Mittaz, J., Merchant, C. J. and Woolliams, E. R. (2019) Applying principles of metrology to historical Earth observations from satellites. Metrologia, 56 (3). ISSN 0026-1394 doi: https://doi.org/10.1088/1681-7575/ab1705

8. Revision History

31/7/2019 – This is a new dataset and document.